

Original scientific paper

ADHESIVE CONTACT SIMULATION OF ELASTIC SOLIDS USING LOCAL MESH-DEPENDENT DETACHMENT CRITERION IN BOUNDARY ELEMENTS METHOD

UDC 531.2

Roman Pohrt¹, Valentin L. Popov^{1,2}

¹Berlin Institute of Technology, Germany

²National Research Tomsk State University, Russia

Abstract. *Using the concept of stress intensity factors, we suggest a way to include adhesion into boundary elements simulation of contacts. A local criterion concerning the maximum admissible surface stresses decides whether the adhesive bonds in particular grid points fail or not. By taking into account the grid spacing, a robust methodology is found. Validation is done using the theoretically derived cases of JKR adhesion.*

Key Words: *Boundary Element Method, Adhesion Simulation, JKR, Detachment*

1. INTRODUCTION

When two arbitrary bodies enter into contact, they exert relatively weak attracting forces, which rapidly decrease with increasing distance. This sticking is called adhesion and plays an important role in many technical applications such especially glue and adhesive tapes. In general, adhesion comes into play when one of the following conditions is met. Either the surfaces are very smooth, or one of the contacting bodies is made of a very soft material. In both cases, this allows for a wide-spread intimate contact. Adhesive effects are also increased when the system size is small due to the different scaling of volume- and surface- forces. For example, in micromechanical devices (MEMS), engineers must design clearances and stiffnesses in such a way that the structures stay movable and do not interlock due to adhesion. The same effect is exploited in biological systems, such as the sticking pads of insects or lizards. For the understanding and prediction of such systems, an appropriate description is needed. From a theoretical point

Received January 09, 2015 / Accepted February 12, 2015

Corresponding author: Pohrt, Roman

Technische Universität Berlin, Straße des 17. Juni 135, 10623 Berlin, Germany

E-mail: roman.pohrt@tu-berlin.de

of view, two influential approaches have been developed in order to describe adhesive contacts for the basic case of elastic, parabolic bodies. Johnson, Kendal and Roberts [1] (JKR), took into account the adhesion forces within the contact area. They calculated the contact radius in the equilibrium state from the minimum in the total energy, which is, in turn, obtained from the elastic deformation energy, the potential of external forces, and the surface energy of the contacting bodies. Derjaguin et al. [2] (DMT theory) considered the molecular forces of attraction only within a ring outside the contact area. Even though these forces contribute to the macroscopic attracting force, they are assumed to cause no deformation. The predicted maximum adhesion force coincides with the one given by Bradley [3] for the contact between rigid spheres.

This discrepancy between the JKR and the DMT theories was finally resolved by Tabor [4] who successfully formulated two different regions of validity for both cases, based on a dimensionless parameter. Accordingly, the DMT theory applies to small, rigid spheres, while the JKR theory is more appropriate for describing large, soft spheres. Later, Johnson and Greenwood [5] pointed out the fact that the JKR theory still provides good results outside its actual area of validity. Over the years, JKR theory has evolved to be the most widely used in the description of adhesion.

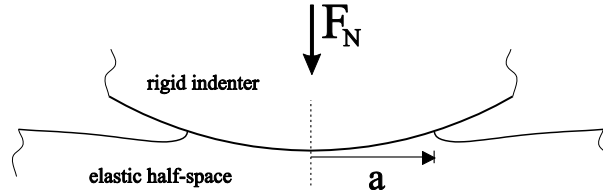


Fig. 1 Qualitative presentation of an adhesive contact between a rigid, curved body and an elastic half-space

2. LOCAL CRITERION IN BEM

Assume two non-conforming bodies $z_1(x,y)$, $z_2(x,y)$ in contact. Elastic deformations $u_z(x,y)$ inside the resulting contact zone must satisfy the condition

$$z_1(x, y) - z_2(x, y) + u_z(x, y) = 0 \quad (1)$$

in order to account for non-overlapping. The necessary surface stress can only occur inside the contact region and, for bodies with smooth geometries, it will vanish at the contact border. When the bodies keep the same contact area, but are pulled apart by distance d , then all the surface points within the contact area are deformed by that constant distance d and the deformation now reads

$$z_1(x, y) - z_2(x, y) + u_z(x, y) + d = 0. \quad (2)$$

In the case of a circular contact area, additional stress σ which arises from the constant deformation by distance d , is given by

$$\sigma = \frac{E^* d}{\pi} (a^2 - r^2)^{-1/2}. \quad (3)$$

Here $E^* = [(1-\nu_1^2)/E_1 + (1-\nu_2^2)/E_2]^{-1}$ is the reduced modulus of elasticity with E being the Young's modulus and ν the Poisson ratio of the two bodies, respectively. The stress intensity factor from Eq. (3) is given by [7]

$$K_I = \frac{E^* d}{\sqrt{\pi a}} = \sqrt{2E^* \Delta\gamma}, \quad (4)$$

where $\Delta\gamma$ is the effective adhesion energy after Dupré for two surfaces. For other contact zone geometries we expect also a singularity of this type

$$\sigma(x) = \sigma_0 \sqrt{L/x}, \quad (5)$$

similar to the theory of fracture mechanics. Here x is a coordinate in the interface plane perpendicular to the contact boundary, starting from the same and pointing into the material. L and σ_0 are characteristic length and stress. This singular curve applies, as long as we are sufficiently close to the contact border, which corresponds to the crack tip (see Fig. 2). In fracture mechanics, as well as adhesion theory, this rise in local stresses leads to a detachment of the bodies and thereby moves the crack tip or decreases the contact zone.

In a numerical representation of stresses, this singularity, Eq. (5), is a problem for two reasons. First, the discretized grid is limited in its resolution and can only approach the contact border with a certain precision. Second, numerical number representation is limited as well and cannot take into account very high values [6]. We will now suggest a way of overcoming these difficulties using a local, mesh dependent detachment criterion.

Let h be the grid spacing, the distance between two points on the numerical mesh.

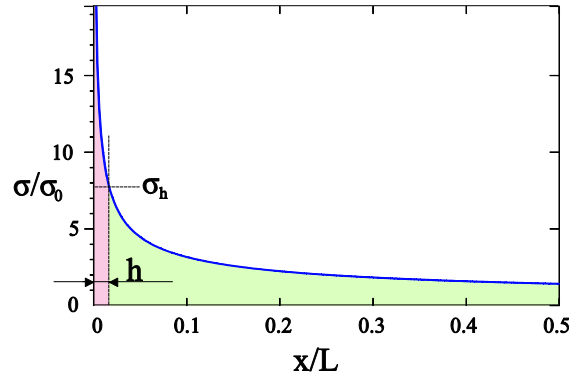


Fig. 2 Singularity (5) at the contact area boundary. By requesting points to have $\sigma < \sigma_h$, it is guaranteed for these points to be inside the contact zone by at least distance h (the grid spacing)

Assume a singularity according to Eq. (5). Even though the exact description of the singularity and the border is not possible using discretized grid and number format, we can safely state that any point in the vicinity of the boundary which has tensile stress below

$$\sigma_h = \sigma_0 \sqrt{L/h} \propto h^{-1/2} \quad (6)$$

is at least distance h away from the singularity and should adhere in any case. Any stress greater than σ_h , the grid point is located ‘at’ the boundary, with the precision of the chosen grid. If we wish to find a local stress criterion Σ for detachment, it is clear that such a criterion must scale with $h^{-1/2}$ just like σ_h . Concerning materials parameters E^* and $\Delta\gamma$, the criterion must scale in the same way as stress intensity factor K_I . In order to find the correct value and factor, let us consider another perspective. A rectangular grid element can only detach when its stored elastic energy U_{el} exceeds the separation energy U_{surf} . For a rectangular grid with dimensions $h_x \times h_y$ the latter is simply given by

$$U_{surf} = h_x h_y \Delta\gamma. \quad (7)$$

The elastic energy stored in a grid element can generally be obtained from

$$U_{el} = \frac{1}{2} \iint \sigma u dA, \quad (8)$$

where u is the deformation resulting from surface stress σ . With Boussinesq

$$u(x, y) = \frac{1}{\pi E^*} \iint \frac{\sigma(\tilde{x}, \tilde{y})}{\sqrt{(x-\tilde{x})^2 + (y-\tilde{y})^2}} d\tilde{x} d\tilde{y}, \quad (9)$$

and the basic BEM assumption that the pressure inside the element is constant, this gives

$$U_{el}(\tau) = \frac{\sigma^2}{2\pi E^*} \int_0^{h_x} \int_0^{h_y} \int_0^{h_x} \int_0^{h_y} \frac{1}{\sqrt{(x-\tilde{x})^2 + (y-\tilde{y})^2}} d\tilde{x} d\tilde{y} dx dy = \frac{\sigma^2}{E^*} \chi. \quad (10)$$

After some algebra we find

$$\begin{aligned} \chi = & \frac{1}{3\pi} (h_x^3 + h_y^3 - h_x^2 \bar{h} - h_y^2 \bar{h}) \\ & + \frac{1}{2\pi} h_x h_y \left[h_x \log \left(\frac{\bar{h} + h_y}{\bar{h} - h_y} \right) + h_y \log \left(\frac{\bar{h} + h_x}{\bar{h} - h_x} \right) \right] \end{aligned} \quad (11)$$

where $\bar{h} = \sqrt{h_x^2 + h_y^2}$. In the common case of square grid elements $h = h_x = h_y$, Eq. (11) reduces to

$$\chi = h^3 \frac{2}{3\pi} \left(1 - \sqrt{2} + \frac{3}{2} \log \left(\frac{\sqrt{2} + 1}{\sqrt{2} - 1} \right) \right) \approx 0.473201 h^3 \quad (12)$$

Demanding that $U_{el} = U_{surf}$ for $\sigma = \Sigma$ we can compare Eq. (7) and Eq. (10) to define a grid-dependent, critical stress value

$$\Sigma = \sqrt{\frac{h_x h_y}{\chi} E^* \Delta\gamma}. \quad (13)$$

Or for square grid elements

$$\Sigma = \sqrt{\frac{E^* \Delta\gamma}{0.473201 \cdot h}} \quad (14)$$

The requirement is that no single tensile stress value solved for a local grid point must exceed Σ .

In a numerical procedure, this can be handled in the following way. Assume we have the adhesion-free normal indentation of the indenter solved (see [8]). Now we wish to decrease the indentation depth from d_{max} to d . The procedure is done as depicted in Fig. 3. In the first step, contact area A is left unchanged and the stresses are solved which are necessary for eliminating the gap between the bodies. This can be done using the techniques described in [8]. The discrete stresses are individually compared to Σ . All the points where this value is exceeded by tensile stress are excluded from the contact zone and the system is solved again. The loop of the algorithm is used to find the correct real contact area.

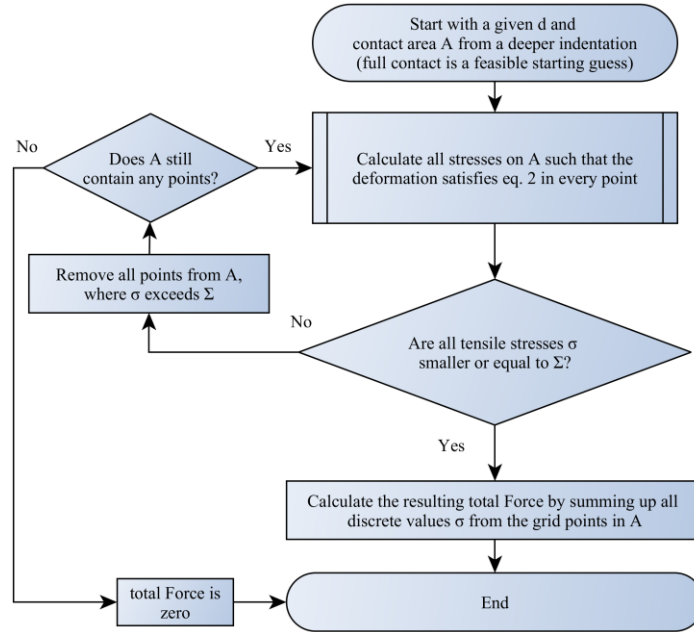


Fig. 3 Flow chart of adhesion algorithm

For every iteration, we must recalculate all the stresses inside the contact area. It is potentially a time-consuming procedure but the contact area can only decrease, so the algorithm is guaranteed to terminate.

3. NUMERICAL SAMPLE STUDIES

In this section we will show that the methodology proposed in section 2 can be effectively used to simulate the adhesive detachment of bodies in contact. Several test cases exist, where analytical solutions are available. In order to illustrate the application of this rule, we will first consider the adhesive contact between a flat, cylindrical indenter with radius R and an elastic half-space. In this case physically, the whole contact zone will detach simultaneously. The total normal force required to separate the indenter from the substrate is then [9]

$$F_{adh} = \sqrt{8\pi a^3 E^* \Delta\gamma} \quad (15)$$

The critical value for the (negative) indentation depth at the moment of detachment is given by

$$d_{crit} = \frac{F_{adh}}{2aE^*} = \sqrt{\frac{2\pi a \Delta\gamma}{E^*}} \quad (16)$$

Fig. 1 shows the resulting forces for a decreasing indentation depth. It can be seen that as d approaches d_{crit} , the force approaches F_{adh} Eq. (15) and then suddenly falls to zero (see arrow). At F_{adh} , also the whole contact is suddenly lost, as depicted in Fig. 1 (b).

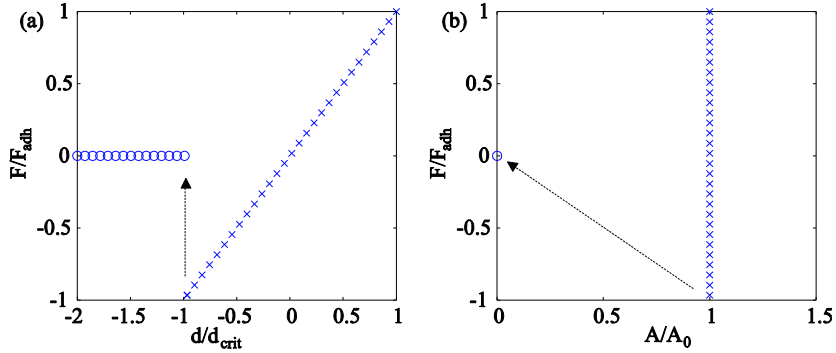


Fig. 4 Numerical pull-off of a flat cylindrical indenter. Crosses demark points where no local detachment is found, circles show points where at least one grid point has lost contact. (a) normal force over indentation (b) normal force over contact area

Let us now test the classical JKR case of a parabola indented into the elastic half space. At the critical point with maximum adhesive force, the theory states [9]

$$F_{adh} = \frac{3}{2} \Delta\gamma\pi R, \quad a_{crit} = \left(\frac{9\pi}{8} \frac{\Delta\gamma R^2}{E^*}\right)^{1/3}, \quad d_{crit} = -\left(\frac{3\pi^2}{64} \frac{\Delta\gamma^2 R}{E^{*2}}\right)^{1/3} \quad (17)$$

Starting from a deeper indentation, the dependencies between normalized indentation depth $\tilde{d} = d/|d_{crit}|$, normal Force $\tilde{F} = F/|F_{adh}|$, and contact radius $\tilde{a} = a/a_{crit}$ read [9]

$$\tilde{d} = 3\tilde{a}^2 - 4\tilde{a}^{1/2} \quad (18)$$

and

$$\tilde{F} = \tilde{a}^3 - 2\tilde{a}^{3/2}, \quad \tilde{F} \approx 0.12(\tilde{d}+1)^{5/3} - 1. \quad (19)$$

In Fig. 5 and Fig. 6 these dependencies are shown with solid lines.

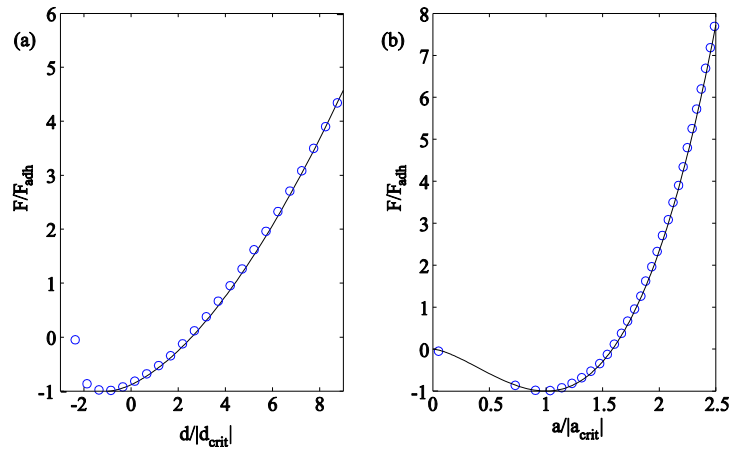


Fig. 5 Numerical indentation-controlled pull-off of an adhesive contact with a parabola. The grid resolution is 128×128 points. Crosses demark points where no local detachment is found, circles show points where at least one grid point has lost contact. (a) normal force over indentation (b) normal force over contact radius

The calculation time of the overall procedure depends very much on the implementation of the stress-finding subprocedure, which usually has complexity N_g^2 , where N_g is the number of grid points in one direction.

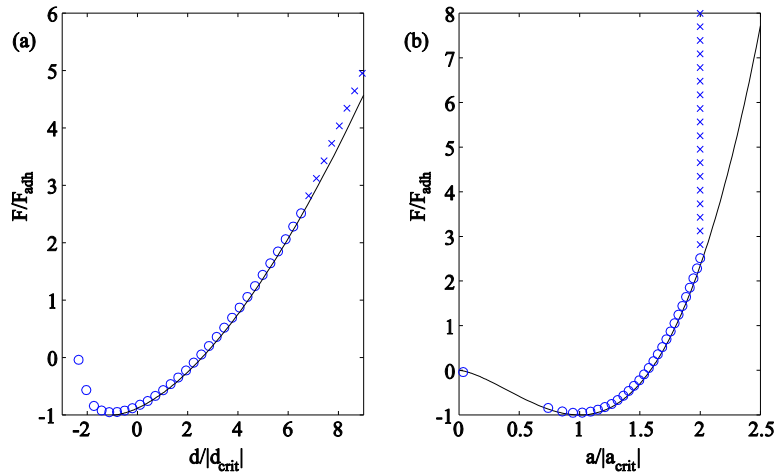


Fig. 6 Numerical indentation-controlled pull-off of an adhesive contact with a parabola. The grid resolution is 512×512 points. Crosses demark points where no local detachment is found, circles show points where at least one grid point has lost contact. In contrast to the case shown in Fig. 5, this time the initial indentation is the Hertzian case with no prior pull-off. Therefore, tensile stresses must first build up at the boundary, before some detachment occurs. (a) normal force over indentation (b) normal force over contact radius

As points are individually excluded from the contact zone, increasing the grid resolution also increases the number of iterations used. Empirically, we have found the computational time to scale with $\propto N_g^{5/2}$ and $\propto N_d^{0.55}$, where N_d is the number of intermediate indentation steps. In our setup, a full JKR solution as in Fig 5. took 106 seconds with a grid of 256×256 ($N_g = 256$) and $N_d = 45$.

4. CONCLUSION

Similar to crack propagation, simulating the adhesive normal contact problem is difficult because it generally has a singularity at the boundaries. When treating the problem numerically, it has been unclear how to find the correct boundary and how to deal with the finite resolution that is available. We suggest a very simple stress-based criterion to be included in BEM simulations. Whenever the criterion is not satisfied, the particular points are removed from the contact zone. Using two examples with known analytical solutions, we show that this approach can successfully simulate the pull-off of adhesive contact. Plasticity is not taken into account. The method shown here can be combined with other BEM techniques, in order to simulate roughness, viscoelastic materials or frictional effects. Readers who wish to implement the new methodology can do so using the instructions given here and in [8].

Acknowledgements: *One of the authors (R. Pohrt) received funding from project PO 810/22-1 by Deutsche Forschungsgemeinschaft. This work is supported in part by Tomsk State University Academic D.I. Mendeleev Fund Program.*

REFERENCES

1. Johnson, K. L., Kendall, K., Roberts, A. D., 1971, *Surface energy and the contact of elastic solids*, Proc. R. Soc. Lond. A, 324 (1558), pp. 301-313.
2. Derjaguin, B. V., Muller, V. M., Toporov, Y. P., 1975, *Effect of contact deformation on the adhesion of particles*, Journal Colloid Interface Sci., 55, pp. 314-326.
3. Bradley, R. S., 1932, *The cohesive force between solid surfaces and the surface energy of solids*, Philos. Mag., 13, pp. 853-862.
4. Tabor, D., 1977, *Surface forces and surface interaction*, J. Colloid Interface Sci., 58, pp. 2-13.
5. Johnson, K. L., Greenwood, J. A., 1997, *An adhesion map for the contact of elastic spheres*, J. Colloid Interface Sci., 192, pp. 326-333.
6. Kuna, M., 2008, *Numerische Beanspruchungsanalyse von Rissen*, Vieweg+Teubner.
7. Popov, V.L., Heß, M., 2015, *Method of Dimensionality Reduction in Contact Mechanics and Friction*, Springer.
8. Pohrt, R., Li, Q., 2014, *Complete Boundary Element Formulation for Normal and Tangential Contact Problems*, Physical Mesomechanics, 17(3), pp. 1-12.
9. Popov, V. L., 2010, *Contact Mechanics and Friction. Physical Principles and Applications*, Springer.